Computational and Theoretical Chemistry 1189 (2020) 112980

Contents lists available at ScienceDirect

Computational and Theoretical Chemistry

journal homepage: www.elsevier.com/locate/comptc

Chitosan/graphene oxide composite as an effective removal of Ni, Cu, As, Cd and Pb from wastewater

Abdelrhman A. Menazea[a,b,*], Hend A. Ezzat[c], Wessam Omara[d,e], Osama H. Basyouni[e,f], Samah A. Ibrahim[g], Aya A. Mohamed[h], Walid Tawfik[i], Medhat A. Ibrahim[b]

[a] Laser Technology Unit, National Research Centre, 12622 Dokki, Giza, Egypt
[b] Spectroscopy Department, National Research Centre, 12622 Dokki, Giza, Egypt
[c] Nano Technology Unit, Solar and Space Research Department, National Research Institute of Astronomy and Geophysics (Nano NRIAG), 11421 Helwan, Cairo, Egypt
[d] Materials Science Department, Institute of Graduate Studies and Research, Alexandria University, 21526 Alexandria, Egypt
[e] Egypt Nanotechnology Center, Cairo University, El-Sheikh Zayed, 6th October, 12588 Giza, Egypt
[f] Department of Physics, Faculty of Science, Kafrelsheikh University, 33516 Kafrelsheikh, Egypt
[g] Physics Department, Special Physics Branch, Faculty of Science, Ain Shams University, 11566 Cairo, Egypt
[h] Department of Physics, Faculty of Science, Cairo University, Cairo, Egypt
[i] National Institute of Laser NILES, Cairo University, Cairo, Egypt

ARTICLE INFO

Keywords:
Chitosan
Graphene Oxide
Heavy metal removal
LANL2DZ

ABSTRACT

The possible interactions between some divalent heavy metals and chitosan/graphene oxide (Cs/GO) were studied by density functional theory (DFT) at B3LYP level with LANL2DZ basis set. Ni, Cu, As, Cd and Pb have been selected as the heavy metals to be studied because of their high impact in industrial wastewater. The interactions between Cs and these heavy metals have been considered and compared to Cs/GO composite. The proposed model was applied to study the interaction between Cs and the heavy metals in compare to both the effect of oxygen-containing groups on the surface of GO and the effect of the nitrogen-containing groups on the surface of Cs. The interaction between the composite Cs/GO and hydrated metal showed more selectivity for the metals than Cs alone. These new results can be applied in the field of environmental pollution by removing the heavy metals from industrial wastewater.

1. Introduction:

Environmental pollution has become a serious problem for the public heath due to increase both of the industrialization cycle and the indiscriminate dumping of heavy metal among many other pollutants [1]. Harmful pollutants in water, such as heavy metals, and chemical dyes represent sources of toxicity and bio-accumulative potential in the food chain [2,3].

The continuous development of novel routes and techniques that capable of providing clean and safe water to humans have become significant interest for scientists [4,5]. These techniques have been determined for extraction toxic metals from wastewater, such as: electrochemical separation [6], reverse osmosis [7], membrane filtration [8], ion exchange [9], coagulation [10], electrochemical deposition [11], pulsed laser ablation [12–15] and pulsed laser deposition (PLD) [16–20].

Among the latter methods, adsorption is the most considerable process in water treatment procedures due to its high performance, easy operation and inexpensive [21]. Owing to its outstanding metal-binding abilities and low-cost, chitosan (Cs) has gained substantial studies area in extraction heavy metals [22]. Besides having biocompatible and biodegradable properties [23,24], the extensive amino and hydroxyl functional groups along its molecular chains, chitosan gains the powerful adsorption capability by forming heavy metal coordination bonds [25]. Chitosan usually demonstrates great water dissolvability and better antibacterial properties. Chitosan's chemical modifications are the true choices for advancing its properties to be implemented in a wide field of water purification [26,27].

In 2014, Deka and Bhattacharyya [28] applied (DFT) B3LYP/6–31 + + G (d, p) for optimization and energy calculations. In 2015, Mokhtari et al. applied [29] (DFT) B3LYP- 6-31G to detect the properties of chitosan functionalized graphene and graphene-oxide systems. Also, in 2015, De Silva and Rajapakse used (DFT) B3LYP- 6-31G (d) basis set employing in a gas phase model, the significant shift in the IR bands in the close vicinity of coordination sites upon metal binding may serve as a diagnostic tool for determining metal binding preferences of

* Corresponding author.
E-mail address: aanter7@gmail.com (A.A. Menazea).

https://doi.org/10.1016/j.comptc.2020.112980
Received 28 April 2020; Received in revised form 21 July 2020; Accepted 5 August 2020
Available online 12 August 2020
2210-271X/

bio-adsorbents such as chitosan [30]. In 2016, Bayat and Akbariyan [31] ab initio HF/6-31G, It wasn't possible to employ a more sophisticated basis set due to the large sizes of the molecules. In 2017, Hassan et al. have analyzed the chitosan and its derivatives using DFT B3LYP method while basis set chosen was LANL2DZ and the optimized global minimum geometry was chosen for metal binding [32]. Since the study considered only the monomeric form, it is useful in certain biological conditions as polymerization is applied to chitosan to obtain the oligosaccharides or monomers. This research work assumed that chitosan is monomer and its derivatives are a good adsorbent for the uptake of Hg (II). In 2019, Ibrahim et al. have performed [33] (DFT) B3LYP- 6-311G++ (d, p) to study the oxidative grafting copolymerization of both 2-hydroxyaniline and 2-methylaniline onto chitosan in the gas phase. Also, in 2019, Mirzaei et al. [34] and Vieira et al. employed [35] applied (DFT) B3LYP-6–311++G and for the representative of atoms C, H, O and LANL2DZ to illustrate pseudopotential for the heavy metals. Their results showed a consistent interaction in the complexation of the carbonyl, hydroxyl and amide groups in CL with both metals [Cu (II) and Pb (II)].

On the other hand, Graphene is single sheet of pure carbon, wrapped in a two-dimensional lattice of crystal [36–38]. It is considered as a good candidate for the adsorption of pollutants from contaminated water is graphene with a high surface area and strong chemical stability [39]. A critical concern, however, is that the graphene still readily aggregates and makes it impossible to spread homogeneously in a matrix [40–43]. Owing to their interesting physical/chemical properties, graphene oxide (GO), a two-dimensional carbon material that contains several functional groups on its basal planes and edges, has reported tremendous excellence as an effective adsorbent for the removal of heavy metals and toxic pollutants from water [44,45].

The oxygenated functional groups can act as binding positions for complexing heavy metals. In addition, the large unique total area accessible also makes GO an excellent candidate for purification of the water [46]. It is suggested that GO may be a suitable adsorbent for removing high-speed and efficiency heavy metals, dyes and organic contaminants [47]. Additionally, GO nanosheets have been reported to have the opportunity for cross-linking interactions with CS framework because GO bears with groups including oxygen and CS have amino groups [48]. The mixture of chitosan and graphene oxide will improve its adsorbent features such as binding power, selectivity, and mechanical properties, which will play an effective role in enhancing heavy metal adsorption performance [49].

Currently many processing techniques for removing heavy metal from waste water such as chemical precipitation [50], membrane separation [51], ion exchange [52], and electrochemical treatment [53], etc., have been used. To date, many materials have been commonly used for treating wastewater, including activated carbons [54], clay minerals [55], polymers [56], zeolites [57] and mesoporous materials [58]. However, most of the materials referred to above have had issues with poor or defective sorption capacities at low or high pH. Due to its good adsorbance ability and high surface areas, graphene oxide (GO) has become a hot spot for environmental experts worldwide, among the most representative carbon nanomaterials in the last years [59]. Graphene, with a single atomic carbon sheet, has a thickness of 0.334 nm and a theoretical maximum surface area of 2630 m^2g^{-1} [60] as a hexagonally arrayed sp^2 structure. A big graphene derivative, graphene oxide (GO) has demonstrated its abundance of functional groups and exceptional mechanical force to be the prospective substrate for preconcentration of heavy metals [61]. GO has a major advantage in particular in the removal from aqueous alternatives of different heavy metals, such as lead Pb (II) [62] copper Cu (II) [63], cobalt Co (II) [64], Cadmium Cd (II) [65], Cr (VI) [66]. However, there are strong interfunctional bonds between graphene sheets which result in inactive surface chemical properties, lower surface area and poor aqueous solutions dispersion, reduced adsorption efficiency and further use in wastewater treatment [67]. To overcome these disadvantaged, chemical modification of graphene oxide is needed, including the manufactures of GO/metal oxide composites, GO/organic composites and GO/photocatalytic composites are systematic to enrich and extract various heavy metals from wastewater. While these major advances have been achieved, GO-based composites remain confronted with a range of key challenges: (i) GO-based composite interaction mechanisms with heavy metals are still uncertain because of the various surface features of different GO-based composites; (ii) tremendous efforts to recover and reuse GO composites are required because of their high dispersion in aqueous solutions and their close interaction with functions; (iii) it still has a very difficult task to be fully aware of low cost, high volumes and environmentally safe manufacturing processes as low cost and large-scale synthesis continue to be crucial to practical application. In 2019, Hernandes et al. [68] used basis set 6–31 + G (d, p) for the C, H, N and O atoms whereas the basis set LANL2DZ was used for the Cd^{2+}, Cr^{3+}, Cu^{2+}, Hg^{2+}, Pb^{2+}, and Zn^{2+} metal ions. Recently, both Yadav et al. [69] and Bayoumy et al. [70] applied (DFT) B3LYP/6-31G (d) for graphene Oxide and GQDs with CS. (B3LYP) was conducted in this performed calculations where it provides a suitable representation of the electronic structure of graphene-derivatives.

Molecular modeling at different level of theories is a class of computational work show potential for describing the physical and chemical behavior of many systems and molecules covering many field of applications [71–73]. Modeling could provide data for systems and molecules whereas the experimental techniques are limited and/or unavailable.

Accordingly, one can apply the computational methods as an effective tool to study the possible interaction between metals and chitosan modified with graphene oxide. Based upon these considerations, the correlation between Cs/GO and some divalent heavy metals (Pb, Cd, and Ni) which commonly found in industrial wastewater in Egypt. This study is performed molecular modeling to study the electronic properties of Cs/GO with hydrated heavy metals. The density functional theory has been applied, at B3LYP level together with the basis set LANL2DZ. The mechanism of interaction between model molecules and hydrated metals are indicated.

2. Computational details

Chitosan model is chosen as effective tool for heavy metal elimination from aquatic media and the effect of using Graphene Oxide (GO) with chitosan for the same goal. Simulating structures were assumed as adsorption interaction of Cs with hydrated heavy metals and adsorption of Cs/GO with hydrated heavy metals where heavy metals were represented by Ni, Cu, As, Cd and Pb. GAUSSIAN09 program [74] were utilized for calculations at Spectroscopy Department, National Research Centre, Egypt. Calculations computed using DFT theory at B3LYP level [75–77] with LANL2DZ basis set. Each structure is subjected to optimization till reach a minimum local energy value. Upon the calculated structures the HOMO-LUMO band gap energy calculated and also total dipole moment (TDM) with identical theory. Contour Molecular Electrostatic potential (MESP) also computed for all structures.

3. Results and discussion

3.1. Model structure and HOMO-LUMO calculations

Chitosan as biodegradable biopolymer with unique hydrogen bonding is presented as a model for heavy metal removal. The model consists of three units as row material and its interaction with heavy metals by means of Ni, Cu, As, Cd and Pb. Furthermore, each metal is hydrated with five water molecules. To study effect of using GO to enhance Cs properties to be used as heavy metals removal, model structure represents GO, Cs/GO and CS/GO interaction with hydrated metals as Ni, Cu, As, Cd and Pb. Fig. 1 shows models and HOMO-LUMO

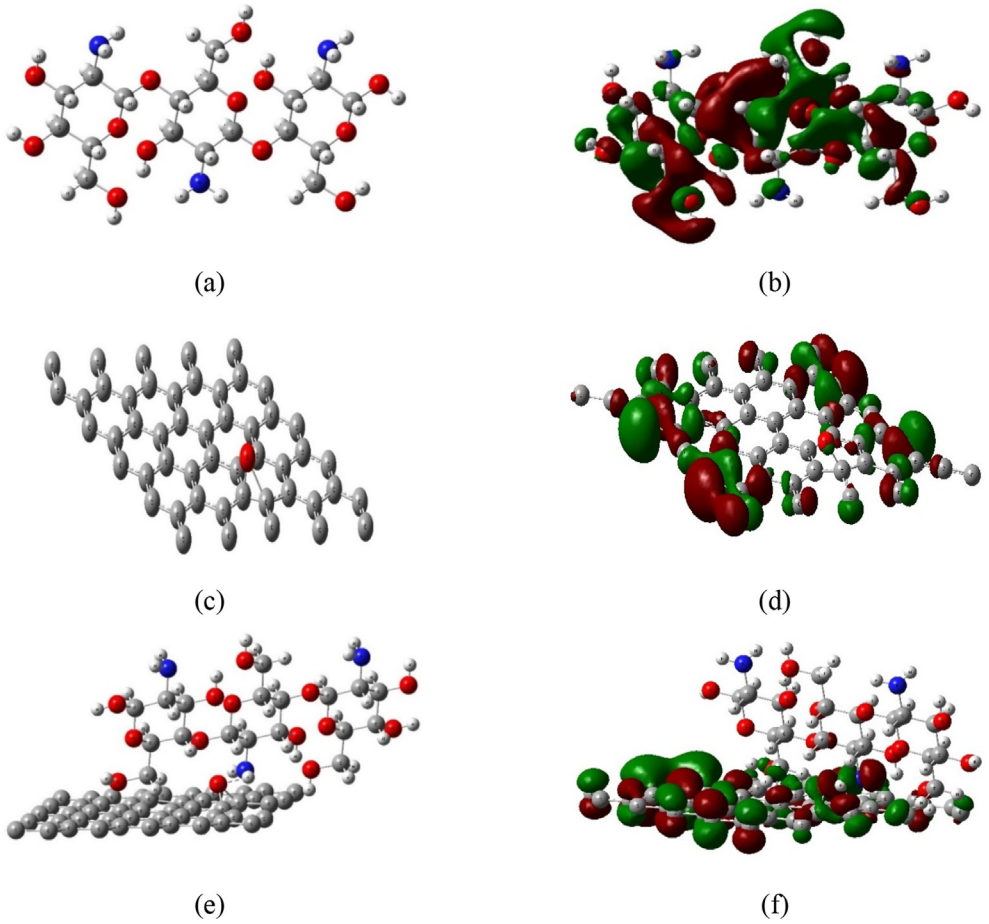

Fig. 1. Optimized models and HOMO-LUMO band gap energy calculated using DFT theory at B3LYP level with LANL2DZ basis set: (a, b) for Cs, (c, d) for GO, (e, f) for Cs/GO, respectively.

Table 1
Optimized TDM (Debye) and HOMO-LUMO band gap energy ΔE (eV) values using DFT theory at B3LYP level with LANL2DZ basis set for Cs, Cs + Ni, Cs + Cu, Cs + As, Cs + Cd, Cs + Pb, GO, Cs/GO, Cs/GO + Ni, Cs/GO + Cu, Cs/GO + As, Cs/GO + Cd and Cs/GO + Pb.

Structure	TDM	ΔE
Cs	4.0949	2.5712
Cs + Ni	13.2800	0.3505
Cs + Cu	23.4435	0.4942
Cs + As	24.4467	0.5644
Cs + Cd	5.4632	0.9807
Cs + Pb	27.8240	0.3464
GO	2.7105	0.4498
Cs + GO	39.5935	0.4114
Cs + GO + Ni	75.8117	0.3725
Cs + GO + Cu	64.3816	0.3279
Cs + GO + As	54.9783	0.3132
Cs + GO + Cd	65.4845	0.3050
Cs + GO + Pb	71.4807	0.2761

band gap energy for Cs, GO and GO with Cs respectively. Structures were calculated using DFT theory [78–81] at B3LYP level with LANL2DZ basis set. Symmetrical distribution orbitals around molecules illustrated. HOMO-LUMO band gap energy and total TDM for supposed Cs, GO and Cs/GO as row materials were estimated at the same level of theory as shown in Table 1. Both TDM and HOMO-LUMO band gap energy recorded for Cs equal 4.094 Debeye and 2.571, for GO equal 2.7105 and 0.4498 and for Cs/GO equal 39.594 and 0.411 respectively. Accordingly, TDM for CS/GO increased and ΔE decreased that Cs affected by GO addition.

Calculated physical parameters are closely correlated with the reactivity of the studied structures. As stated earlier physical quantities such as total dipole moment TDM and HOMO/LUMO bang gap energy could be correlated with the reactivity of a given compound. The structure is reactively interact with its surrounding media as its TDM increased while its HOMO/LUMO band gap is decreased [82,83]. The Molecular electrostatic potential is considered as another measure for the reactivity as it indicated the sites enable the structure to interact with its surrounding molecules [84–86].

3.2. Chitosan with hydrated metals

Chitosan interaction with hydrated metals was supposed as Cs + M with the existence of $5H_2O$ were M where Ni, Cu, As, Cd and Pb. HOMO-LUMO band gap energy and TDM were computed at the same level of theory for all model molecules. Models of Cs and Cs + M and its HOMO-LUMO band gap energy were simulated in Fig. 2 respectively. From Fig. 2, Cs orbital distribution affected by metal interaction.

As listed in table 1, TDM and ΔE band gap energy values also suffered from changes according to the interaction with metal. Accordingly, Cs + Ni TDM increased to 13.280 Debye and ΔE decreased to 0.350 which means that Ni effect on Cs. Furthermore, Cs + Cu TDM increased to 23.444 Debye and ΔE decreased to 0.494 eV. TDM changed as 24.447 Debye and ΔE as 0.564 eV according to As interaction with Cs. Similarly, Cs + Cd TDM and changed to 5.463 Debye and ΔE to 0.981 eV respectively. Equally, Cs + Pb ΔE and TDM values became 0.346 eV and 27.824 Debye. Changing in TDM directly while ΔE changing inversely, means the high ability for interaction existence.

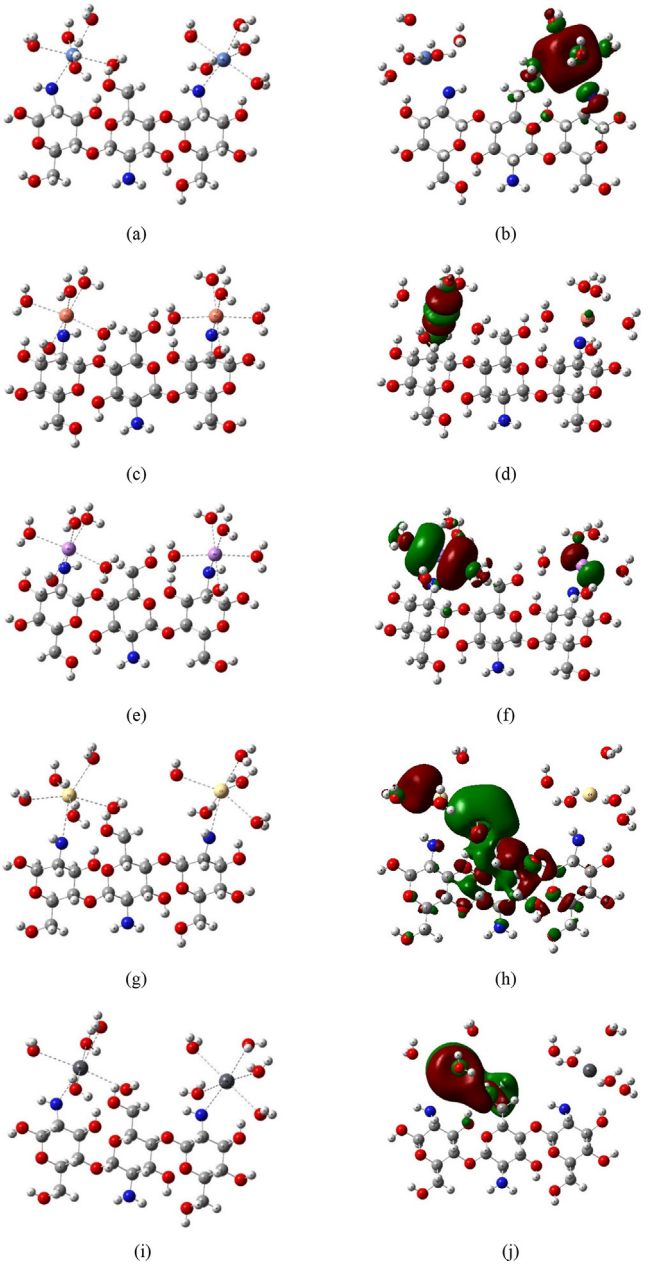

Fig. 2. Optimized models and HOMO-LUMO band gap energy calculated using DFT theory at B3LYP level with LANL2DZ basis set: (a, b) for Cs + Ni, (c, d) for Cs + Cu, (e, f) for Cs + As (g, h) for Cs + Cd, and (i, j) for Cs + Pb, respectively.

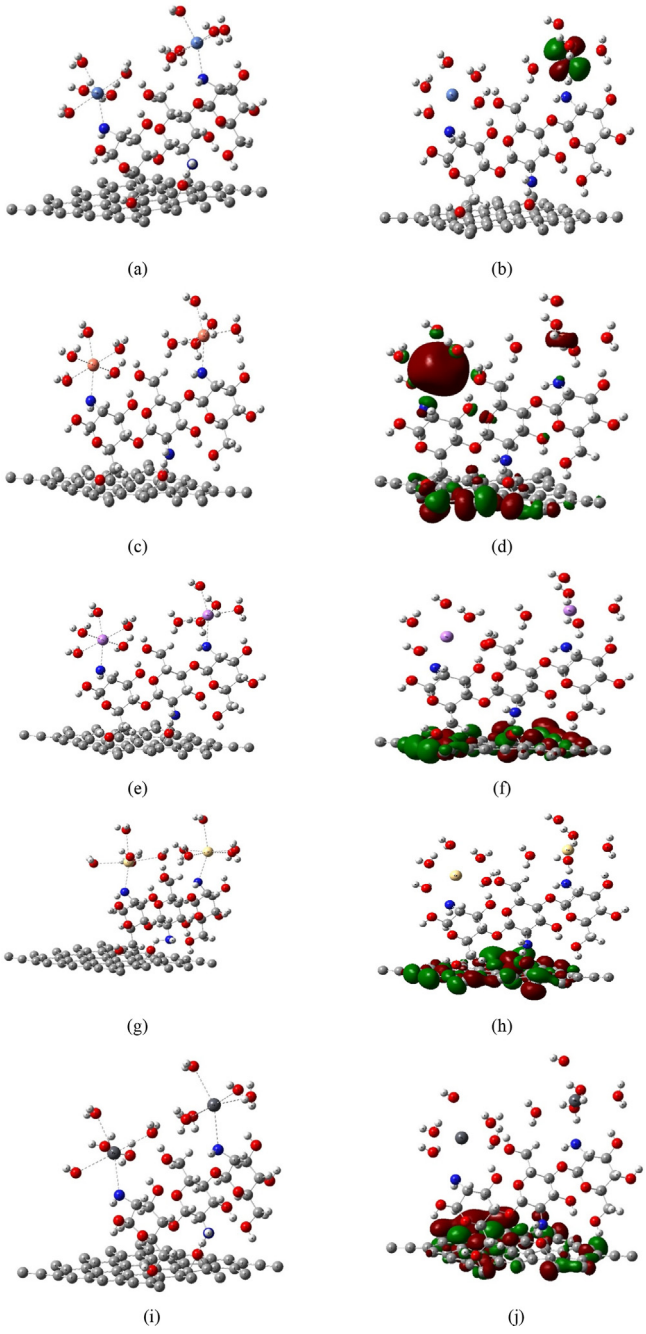

Fig. 3. Chitosan/Graphene Oxide and Chitosan/Graphene Oxide with Hydrated Metals models optimized HOMO-LUMO band gap energy at basis set B3LYP/LANL2DZ: (a, b) for Cs/GO + Ni (c, d) for Cs/GO + Cu, (e, f) for Cs/GO + As, (g, h) for Cs/GO + Cd, and (i, j) for Cs/GO + Pb, respectively.

According to result Nickel and lead having the highest ability to interact with chitosan, which the highest value of TDM and the lowest value of ΔE returned to them.

3.3. Chitosan/graphene oxide with hydrated metal

GO was used to improve the efficiency of Cs for metals attraction by applying model structure of Cs/GO interaction with hydrated metals as Ni, Cu, As, Cd and Pb with the existence of $5H_2O$. HOMO-LUMO band gap energy and TDM were calculated at the same level of theory for all model molecules represented in Fig. 3 respectively. Fig. 3 explores the metals effect on the orbital distribution of Cs/GO.

As mentioned previously in Table 1, TDM and ΔE band gap energy for Cs/GO verified the values changes due to metal interaction. So, Cs/GO + Ni TDM improved directly to 75.8117 Debye and ΔE reversely decayed to 0.3725. Furthermore, Cs/GO + Cu TDM up to 64.3816 Debye while ΔE equal 0.3279 eV. Also, Cs/GO + As TDM changed to 54.9783 Debye and ΔE to 0.3132 eV. Similarly, Cs/GO + Cd TDM up to 65.4845 Debye and ΔE reduced to 0.3050 eV respectively. In the same way, Cs/GO + Pb ΔE and TDM values reached 0.2761 eV and 71.4807 Debye. According to result comparison between Cs with hydrated metals and Cs/GO with hydrated metal, it founded that Cs/GO was more selective for hydrated metals more than Cs only. GO addition to Cs caused an improvement to Cs properties as metal removal.

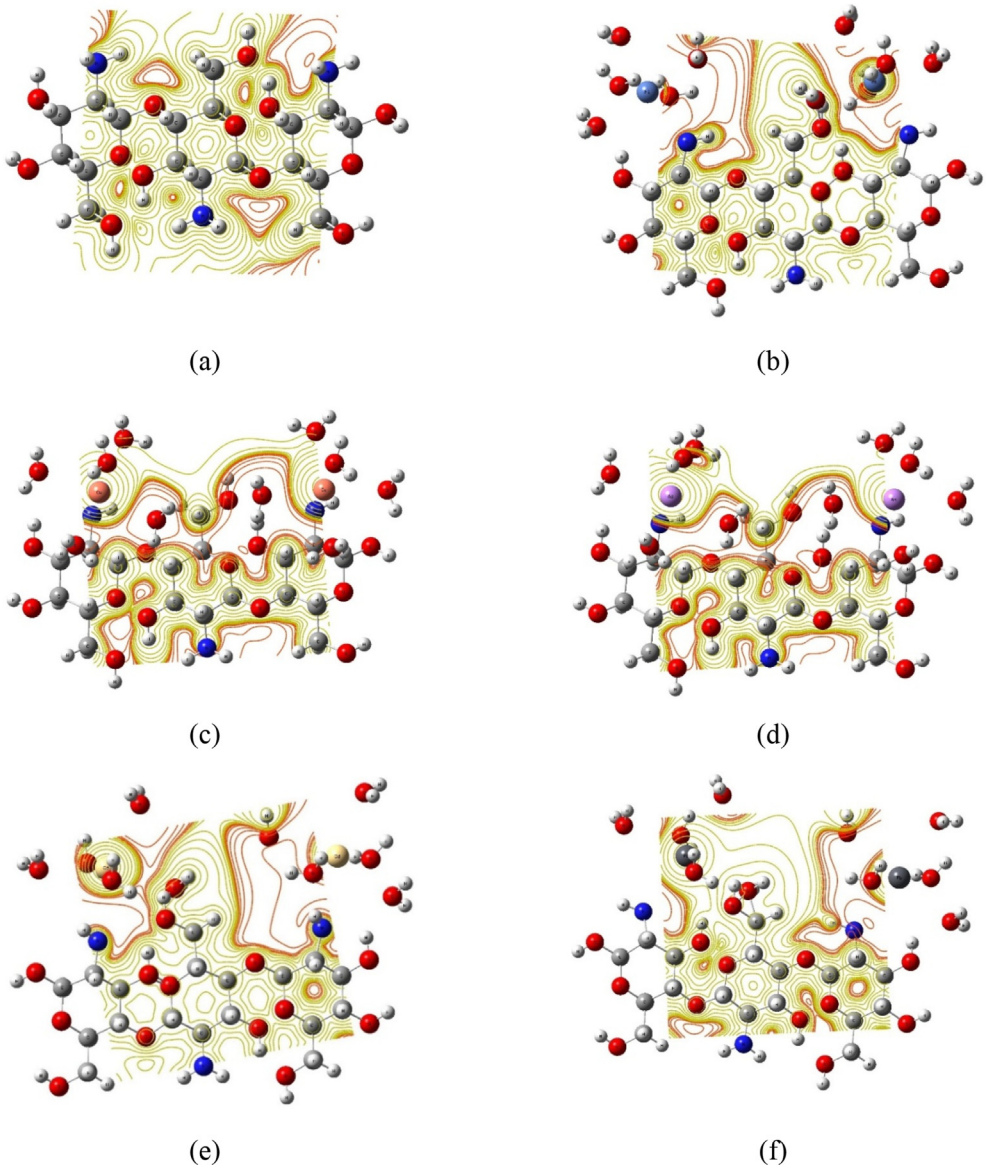

Fig. 4. MESP calculations using DFT theory at B3LYP level with LANL2DZ basis set for (a) Cs, (b) Cs + Ni, (c) Cs + Cu, (d) Cs + As, (e) Cs + Cd, (f) Cs + Pb.

3.4. Molecular electrostatic potential

Molecular electrostatic potential MESP calculations were utilized to understanding all molecular interaction. MESP calculations at same level of theory presented in Figs. 4 and 5 for Cs and its interaction with heavy metals: Ni, Cu, As, Cd and Pb in the existence of 5 water molecules and Cs/GO and its interaction with the same metals at the same conditions. MESP describes charge distribution around the molecule. MESP color spectrum clarified according to extended gradually as Red, orange, yellow, green and blue respectively. Ranged color indication for MESP variation represented as red for the low value and blue for high value. MESP give a prediction about reactivity of molecule according to the negative potential which represent the protonation and nucleophilic sites and positive potential which represent electrophilic sites. The contour MESP indicated that GO gives Cs stability and reactivity for metals Ni, Cu, As, Cd and Pb adsorption.

4. Conclusion

A model describing the possible removal of hydrated heavy metals is presented based on biopolymer modified with graphene oxide. The use GO with Cs designed for the removal of heavy metals from aquatic environment have been studied. Calculations were performed using DFT:B3LYP/LANL2DZ model. The proposed interactions have showed an enhancement in the chitosan properties as heavy metal removal. The observed results indicated that GO improve the stability of Cs and its adsorption reactivity for the metals; Ni, Cu, As, Cd, and Pb. The composite Cs/GO has showed a selectively property for hydrated metals compare to Cs alone. The observed results for our proposed composite Cs/GO showed a correlation for the heavy metals Cd and Pb with Cs which can be applied in the environmental applications as an effective removal of cadmium and lead from wastewater. The present computational study paves the way toward further application of eco-friendly method in future, further experimental verification could be conducted in future for verification and applications of the investigated material.

CRediT authorship contribution statement

A.A. Menazea: Writing - original draft. **Hend Ezzat:** Conceptualization. **Wessam Omara:** Investigation. **Osama H. Basyouni:** Methodology. **Samah A. Ibrahim:** Data curation. **Aya A. Mohamed:** Formal analysis. **Walid Tawfik:** Writing - review & editing.

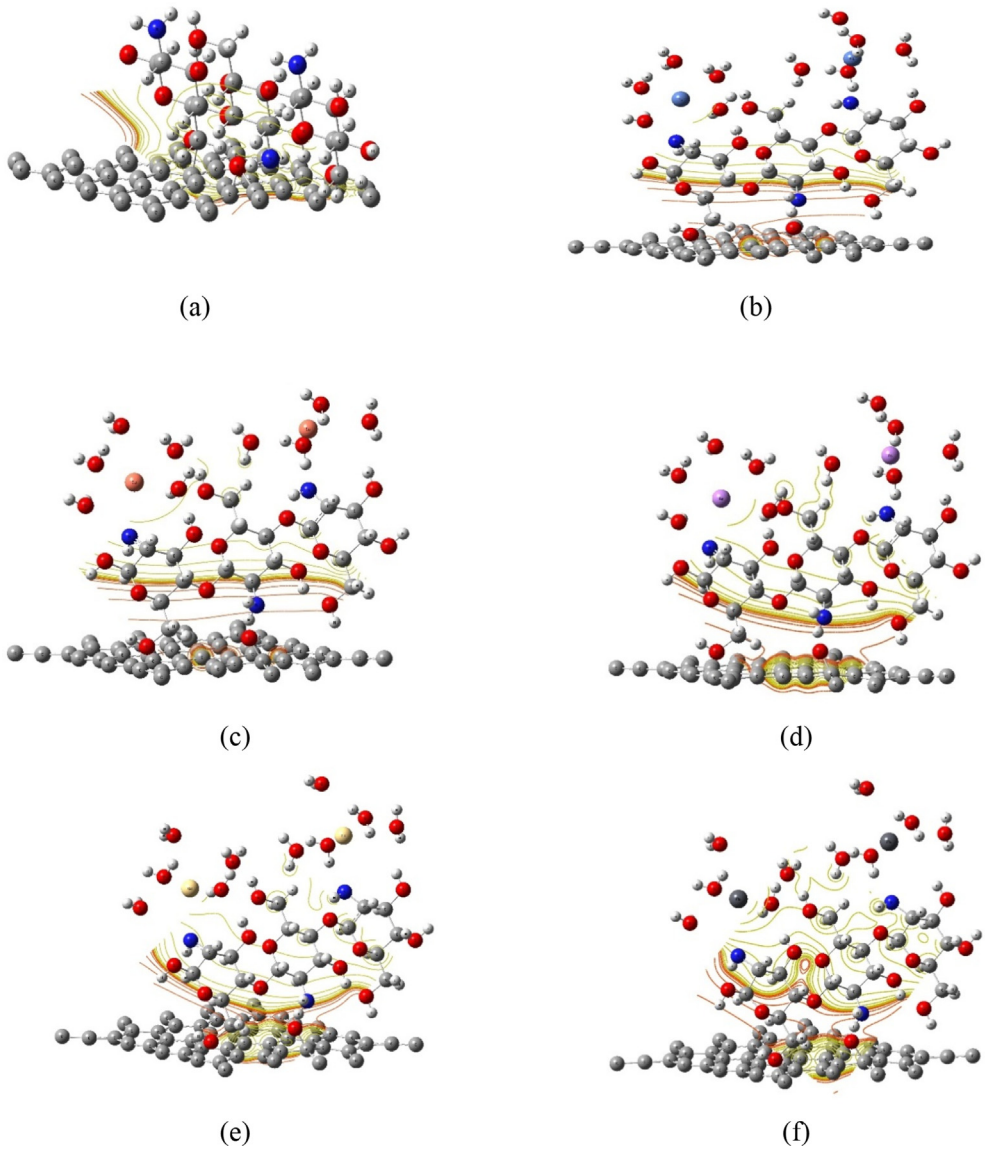

Fig. 5. MESP calculations using DFT theory at B3LYP level with LANL2DZ basis set for (a) Cs/GO, (b) Cs/GO + Ni, (c) Cs/GO + Cu, (d) Cs/GO + As, (e) Cs/GO + Cd, (f) Cs/GO + Pb.

Medhat Ibrahim: Supervision.

Declaration of Competing Interest

The authors declared that there is no conflict of interest.

References

[1] M.A. Moktadir, S.M. Ali, S. Kusi-Sarpong, M.A.A. Shaikh, Assessing challenges for implementing industry 4.0: implications for process safety and environmental protection, Process Saf. Environ. Prot. 117 (2018) 730–741.
[2] S. Ramanayaka, M. Vithanage, A. Sarmah, T. An, K.-H. Kim, Y.S. Ok, Performance of metal–organic frameworks for the adsorptive removal of potentially toxic elements in a water system: a critical review, RSC Adv. 9 (59) (2019) 34359–34376.
[3] B.E. Igiri, S.I.R. Okoduwa, G.O. Idoko, E.P. Akabuogu, A.O. Adeyi, I.K. Ejiogu, Toxicity and bioremediation of heavy metals contaminated ecosystem from tannery wastewater: a review, J. Toxicology 2018 (2018) 1–16.
[4] A. Deshmukh, C. Boo, V. Karanikola, S. Lin, A.P. Straub, T. Tong, D.M. Warsinger, M. Elimelech, Membrane distillation at the water-energy nexus: limits, opportunities, and challenges, Energy Environ. Sci. 11 (5) (2018) 1177–1196.
[5] M.K. Ahmed, M.E. El-Naggar, A. Aldalbahi, M.H. El-Newehy, A.A. Menazea, Methylene blue degradation under visible light of metallic nanoparticles scattered into graphene oxide using laser ablation technique in aqueous solutions, J. Mol. Liq. 315 (2020) 113794, https://doi.org/10.1016/j.molliq.2020.113794.
[6] Q. Tao, X.u. Zhang, K. Prabaharan, Y. Dai, Separation of cesium from wastewater with copper hexacyanoferrate film in an electrochemical system driven by microbial fuel cells, Bioresour. Technol. 278 (2019) 456–459.
[7] E. Sahinkaya, A. Sahin, A. Yurtsever, M. Kitis, Concentrate minimization and water recovery enhancement using pellet precipitator in a reverse osmosis process treating textile wastewater, J. Environ. Manage. 222 (2018) 420–427.
[8] M. Rezakazemi, A. Khajeh, M. Mesbah, Membrane filtration of wastewater from gas and oil production, Environ. Chem. Lett. 16 (2) (2018) 367–388.
[9] I.B. Rae, S. Pap, D. Svobodova, S.W. Gibb, Comparison of sustainable biosorbents and ion-exchange resins to remove Sr^{2+} from simulant nuclear wastewater: Batch, dynamic and mechanism studies, Sci. Total Environ. 650 (2019) 2411–2422.
[10] J. Dotto, M.R. Fagundes-Klen, M.T. Veit, S.M. Palácio, R. Bergamasco, Performance of different coagulants in the coagulation/flocculation process of textile wastewater, J. Cleaner Prod. 208 (2019) 656–665.
[11] M. Lashgari, Y. Yamini, Fiber-in-tube solid-phase microextraction of caffeine as a molecular tracer in wastewater by electrochemically deposited layered double hydroxide, J. Sep. Sci. 41 (11) (2018) 2393–2400.
[12] A.M. Mostafa, E.A. Mwafy, Synthesis of ZnO and Au@ZnO core/shell nano-catalysts by pulsed laser ablation in different liquid media, J. Mater. Res. Technol. 9 (3) (2020) 3241–3248.
[13] A.M. Mostafa, S.A. Yousef, W.H. Eisa, M.A. Ewaida, E.A. Al-Ashkar, WO3 quantum dot: synthesis, characterization and catalytic activity, J. Mol. Struct. 1185 (2019) 351–356.
[14] W.H. Eisa, M.F. Zayed, B. Anis, L.M. Abbas, S.S.M. Ali, A.M. Mostafa, Clean production of powdery silver nanoparticles using Zingiber officinale: The structural and catalytic properties, J. Cleaner Prod. 241 (2019) 118398, https://doi.org/10.1016/j.jclepro.2019.118398.

[15] S. Alghool, H.F. Abd El-Halim, A.M. Mostafa, An eco-friendly synthesis of V2O5 nanoparticles and their catalytic activity for the degradation of 4-nitrophrnol, J. Inorg. Organomet. Polym. 29 (4) (2019) 1324–1330.

[16] A.A. Menazea, A.M. Mostafa, E.A. Al-Ashkar, Impact of CuO doping on the properties of CdO thin films on the catalytic degradation by using pulsed-Laser deposition technique, Opt. Mater. 100 (2020) 109663, https://doi.org/10.1016/j.optmat.2020.109663.

[17] A.M. Mostafa, A.A. Menazea, Laser-assisted for preparation ZnO/CdO thin film prepared by pulsed laser deposition for catalytic degradation, Radiat. Phys. Chem. 176 (2020) 109020, https://doi.org/10.1016/j.radphyschem.2020.109020.

[18] A.A. Menazea, A.M. Mostafa, Ag doped CuO thin film prepared via pulsed laser deposition for 4-nitrophenol degradation, J. Environ. Chem. Eng. 8 (5) (2020) 104104, https://doi.org/10.1016/j.jece:2020.104104.

[19] A.M. Mostafa, E.A. Mwafy, Synthesis of ZnO/CdO thin film for catalytic degradation of 4-nitrophenol, J. Mol. Struct. 1221 (2020) 128872, https://doi.org/10.1016/j.molstruc.2020.128872.

[20] M.A. Zakaria, A.A. Menazea, A.M. Mostafa, E.A. Al-Ashkar, Ultra-thin silver nanoparticles film prepared via pulsed laser deposition: Synthesis, characterization, and its catalytic activity on reduction of 4-nitrophenol, Surf. Interfaces 19 (2020) 100438, https://doi.org/10.1016/j.surfin.2020.100438.

[21] A.M. Mostafa, A.A. Menazea, Polyvinyl Alcohol/Silver nanoparticles film prepared via pulsed laser ablation: an eco-friendly nano-catalyst for 4-nitrophenol degradation, J. Mol. Struct. 1212 (2020) 128125, https://doi.org/10.1016/j.molstruc.2020.128125.

[22] G. Yuvaraja, Y. Pang, D.-Y. Chen, L.-J. Kong, S. Mehmood, M.V. Subbaiah, D.S. Rao, C. Mouli Pavuluri, J.-C. Wen, G.M. Reddy, Modification of chitosan macromolecule and its mechanism for the removal of Pb(II) ions from aqueous environment, Int. J. Biol. Macromol. 136 (2019) 177–188.

[23] M.J. Tommalieh, H.A. Ibrahium, N.S. Awwad, A.A. Menazea, Gold nanoparticles doped polyvinyl alcohol/chitosan blend via laser ablation for electrical conductivity enhancement, J. Mol. Struct. 1221 (2020) 128814, https://doi.org/10.1016/j.molstruc.2020.128814.

[24] A.A. Menazea, A.M. Ismail, N.S. Awwad, H.A. Ibrahium, Physical characterization and antibacterial activity of PVA/Chitosan matrix doped by selenium nanoparticles prepared via one-pot laser ablation route, J. Mater. Res. Technol. 9 (5) (2020) 9598–9606.

[25] S. Ahmed, Annu, A. Ali, J. Sheikh, A review on chitosan centred scaffolds and their applications in tissue engineering, Int. J. Biol. Macromol. 116 (2018) 849–862.

[26] A.A. Menazea, M.M. Eid, M.K. Ahmed, Synthesis, characterization, and evaluation of antimicrobial activity of novel Chitosan/Tigecycline composite, Int. J. Biol. Macromol. 147 (2020) 194–199.

[27] A.M. Abdelghany, A.A. Menazea, A.M. Ismail, Synthesis, characterization and antimicrobial activity of Chitosan/Polyvinyl Alcohol blend doped with Hibiscus Sabdariffa L. extract, J. Mol. Struct. 1197 (2019) 603–609.

[28] B.C. Deka, P.K. Bhattacharyya, Understanding chitosan as a gene carrier: A DFT study, Comput. Theor. Chem. 1051 (2015) 35–41.

[29] A. Mokhtari, K. Harismah, M. Mirzaei, Covalent addition of chitosan to graphene sheets: density functional theory explorations of quadrupole coupling constants, Superlattices Microstruct. 88 (2015) 56–61.

[30] S.M. De Silva, C.S.K. Rajapakse, Use of computational method to identify metal binding sites of chitosan as a tool to investigate the interaction mechanism of chitosan and heavy metals, Proceedings of the Research Symposium of Uva Wellassa University, 2015.

[31] Z. Bayat, N. Akbariyan, Theoretical Study on the Geometrical and physico chemical Properties of Paclitaxel Conjugated to Nanoparticle Chitosan Biopolymer Along with ethylene glycol chains.

[32] B. Hassan, V.K. Rajan, V.M.A. Mujeeb, M. K., A DFT based analysis of adsorption of Hg^{2+} ion on chitosan monomer and its citralidene and salicylidene derivatives: Prior to the removal of Hg toxicity, Int. J. Biol. Macromol. 99 (2017) 549–554.

[33] M.S. Ibrahim, H.A. El-Mageed, H.A. El-Salam, Density functional theory calculations on the grafting copolymerization of 2-substituted aniline onto chitosan, Polym. Bull. (2019) 1–17.

[34] M. Mirzaei, O. Gulseren, E. Jafari, M. Aramideh, A computational molecular approach on chitosan vehicle for metformin, Iranian Chem. Commun. 7 (2019) 380–389.

[35] C.L. Vieira, F.O. Sanches Neto, V.H. Carvalho-Silva, R. Signini, Design of apolar chitosan-type adsorbent for removal of Cu(II) and Pb(II): an experimental and DFT viewpoint of the complexation process, J. Environ. Chem. Eng. 7 (3) (2019) 103070, https://doi.org/10.1016/j.jece:2019.103070.

[36] A. Abbasi, A. Khataee, Band gap tunability and structural stability of metal/non-metal codoped group-IV tin nanotubes: effect of spin-orbit coupling, Physica E 114 (2019) 113644.

[37] M. Corva, A. Ferrari, M. Rinaldi, Z. Feng, M. Roiaz, C. Rameshan, G. Rupprechter, R. Costantini, M. Dell'Angela, G. Pastore, G. Comelli, N. Seriani, E. Vesselli, Vibrational fingerprint of localized excitons in a two-dimensional metal-organic crystal, Nat. Commun. 9 (1) (2018), https://doi.org/10.1038/s41467-018-07190-1.

[38] A. Abbasi, J.J. Sardroodi, Adsorption of O3, SO2 and SO3 gas molecules on MoS2 monolayers: a computational investigation, Appl. Surf. Sci. 469 (2019) 781–791.

[39] L.-Z. Guan, L.i. Zhao, Y.-J. Wan, L.-C. Tang, Three-dimensional graphene-based polymer nanocomposites: preparation, properties and applications, Nanoscale 10 (31) (2018) 14788–14811.

[40] A.A. Menazea, M.K. Ahmed, Synthesis and antibacterial activity of graphene oxide decorated by silver and copper oxide nanoparticles, J. Mol. Struct. 1218 (2020) 128536, https://doi.org/10.1016/j.molstruc.2020.128536.

[41] N. Yousefi, K.K.W. Wong, Z. Hosseinidoust, H.O. Sørensen, S. Bruns, Y.i. Zheng, N. Tufenkji, Hierarchically porous, ultra-strong reduced graphene oxide-cellulose nanocrystal sponges for exceptional adsorption of water contaminants, Nanoscale 10 (15) (2018) 7171–7184.

[42] M.K. Ahmed, S.F. Mansour, R. Al-Wafi, A.A. Menazea, Composition and design of nanofibrous scaffolds of Mg/Se- hydroxyapatite/graphene oxide @ ε-poly-caprolactone for wound healing applications, J. Mater. Res. Technol. 9 (4) (2020) 7472–7485.

[43] A.A. Menazea, M.K. Ahmed, Silver and copper oxide nanoparticles-decorated graphene oxide via pulsed laser ablation technique: Preparation, characterization, and photoactivated antibacterial activity, Nano-Struct. Nano-Objects 22 (2020) 100464, https://doi.org/10.1016/j.nanoso.2020.100464.

[44] V. Nejadshafiee, M.R. Islami, Intelligent-activated carbon prepared from pistachio shells precursor for effective adsorption of heavy metals from industrial waste of copper mine, Environ. Sci. Pollut. Res. 27 (2) (2020) 1625–1639.

[45] J. Xu, Z. Cao, Y. Zhang, Z. Yuan, Z. Lou, X. Xu, X. Wang, A review of functionalized carbon nanotubes and graphene for heavy metal adsorption from water: preparation, application, and mechanism, Chemosphere 195 (2018) 351–364.

[46] A. Bashir, L.A. Malik, S. Ahad, T. Manzoor, M.A. Bhat, G.N. Dar, A.H. Pandith, Removal of heavy metal ions from aqueous system by ion-exchange and biosorption methods, Environ. Chem. Lett. 17 (2) (2019) 729–754.

[47] J. Hao, L. Ji, C. Li, C. Hu, K. Wu, Rapid, efficient and economic removal of organic dyes and heavy metals from wastewater by zinc-induced in-situ reduction and precipitation of graphene oxide, J. Taiwan Inst. Chem. Eng. 88 (2018) 137–145.

[48] C. Qi, L. Zhao, Y. Lin, D. Wu, Graphene oxide/chitosan sponge as a novel filtering material for the removal of dye from water, J. Colloid Interface Sci. 517 (2018) 18–27.

[49] M.S. Samuel, J. Bhattacharya, S. Raj, N. Santhanam, H. Singh, N.D.P. Singh, Efficient removal of Chromium(VI) from aqueous solution using chitosan grafted graphene oxide (CS-GO) nanocomposite, Int. J. Biol. Macromol. 121 (2019) 285–292.

[50] M.S. Oncel, A. Muhcu, E. Demirbas, M. Kobya, A comparative study of chemical precipitation and electrocoagulation for treatment of coal acid drainage wastewater, J. Environ. Chem. Eng. 1 (4) (2013) 989–995.

[51] V. Mavrov, T. Erwe, C. Blöcher, H. Chmiel, Study of new integrated processes combining adsorption, membrane separation and flotation for heavy metal removal from wastewater, Desalination 157 (1-3) (2003) 97–104.

[52] A. Dabrowski, Z. Hubicki, P. Podkościelny, E. Robens, Selective removal of the heavy metal ions from waters and industrial wastewaters by ion-exchange method, Chemosphere 56 (2) (2004) 91–106.

[53] S. Raghu, C.A. Basha, Chemical or electrochemical techniques, followed by ion exchange, for recycle of textile dye wastewater, J. Hazard. Mater. 149 (2) (2007) 324–330.

[54] R. Mailler, J. Gasperi, Y. Coquet, C. Derome, A. Buleté, E. Vulliet, A. Bressy, G. Varrault, G. Chebbo, V. Rocher, Removal of emerging micropollutants from wastewater by activated carbon adsorption: Experimental study of different activated carbons and factors influencing the adsorption of micropollutants in wastewater, J. Environ. Chem. Eng. 4 (1) (2016) 1102–1109.

[55] S.M.R. Shaikh, M.S. Nasser, I. Hussein, A. Benamor, S.A. Onaizi, H. Qiblawey, Influence of polyelectrolytes and other polymer complexes on the flocculation and rheological behaviors of clay minerals: a comprehensive review, Sep. Purif. Technol. 187 (2017) 137–161.

[56] G. Lofrano, M. Carotenuto, G. Libralato, R.F. Domingos, A. Markus, L. Dini, R.K. Gautam, D. Baldantoni, M. Rossi, S.K. Sharma, M.C. Chattopadhyaya, M. Giugni, S. Meric, Polymer functionalized nanocomposites for metals removal from water and wastewater: an overview, Water Res. 92 (2016) 22–37.

[57] J. Wen, H. Dong, G. Zeng, Application of zeolite in removing salinity/sodicity from wastewater: a review of mechanisms, challenges and opportunities, J. Cleaner Prod. 197 (2018) 1435–1446.

[58] W. Huang, Y. Zhang, D. Li, Adsorptive removal of phosphate from water using mesoporous materials: a review, J. Environ. Manage. 193 (2017) 470–482.

[59] J. Ren, C. Wang, X. Zhang, T. Carey, K. Chen, Y. Yin, F. Torrisi, Environmentally-friendly conductive cotton fabric as flexible strain sensor based on hot press reduced graphene oxide, Carbon 111 (2017) 622–630.

[60] S. Yadav, N. Goel, V. Kumar, K. Tikoo, S. Singhal, Removal of fluoroquinolone from aqueous solution using graphene oxide: experimental and computational elucidation, Environ. Sci. Pollut. Res. 25 (3) (2018) 2942–2957.

[61] A.L. Cukierman, A.L. Cukierman, A.L. Cukierman, P.R. Bonelli, P.R. Bonelli, Nanotechnology for Sustainable Water Resources, John Wiley & Sons, Inc., Hoboken, NJ, USA, 2018, pp. 227–276, https://doi.org/10.1002/9781119323655.ch8.

[62] M. Fan, T. Li, J. Hu, R. Cao, Q. Wu, X. Wei, L. Li, X. Shi, W. Ruan, Synthesis and Characterization of Reduced Graphene Oxide-Supported Nanoscale Zero-Valent Iron (nZVI/rGO) Composites Used for Pb(II) Removal, Materials 9 (8) (2016) 687, https://doi.org/10.3390/ma9080687.

[63] G. Zhao, H. Zhang, Q. Fan, X. Ren, J. Li, Y. Chen, X. Wang, Sorption of copper(II) onto super-adsorbent of bentonite–polyacrylamide composites, J. Hazard. Mater. 173 (1-3) (2010) 661–668.

[64] A. Molla, Y. Li, M. Khandelwal, S.H. Hur, J.S. Chung, Anion-controlled sulfidation for decoration of graphene oxide with iron cobalt sulfide for rapid sonochemical dyes removal in the absence of light, Appl. Catal. A 561 (2018) 49–58.

[65] M. Fan, T. Li, J. Hu, R. Cao, X. Wei, X. Shi, W. Ruan, Artificial neural network modeling and genetic algorithm optimization for cadmium removal from aqueous solutions by reduced graphene oxide-supported nanoscale zero-valent iron (nZVI/rGO) composites, Materials 10 (5) (2017) 544, https://doi.org/10.3390/ma10050544.

[66] J. Geng, Y. Yin, Q. Liang, Z. Zhu, H. Luo, Polyethyleneimine cross-linked graphene oxide for removing hazardous hexavalent chromium: Adsorption performance and

mechanism, Chem. Eng. J. 361 (2019) 1497–1510.
[67] X. Liu, R. Ma, X. Wang, Y. Ma, Y. Yang, L.i. Zhuang, S. Zhang, R. Jehan, J. Chen, X. Wang, Graphene oxide-based materials for efficient removal of heavy metal ions from aqueous solution: a review, Environ. Pollut. 252 (2019) 62–73.
[68] I.H.S. Ribeiro, D.T. Reis, D.H. Pereira, A DFT-based analysis of adsorption of Cd^{2+}, Cr^{3+}, Cu^{2+}, Hg^{2+}, Pb^{2+}, and Zn^{2+}, on vanillin monomer: a study of the removal of metal ions from effluents, J. Mol. Model. 25 (9) (2019), https://doi.org/10.1007/s00894-019-4151-z.
[69] S. Yadav, N. Goel, V. Kumar, S. Singhal, Graphene oxide as proficient adsorbent for the removal of harmful pesticides: comprehensive experimental cum DFT investigations, Anal. Chem. Lett. 9 (3) (2019) 291–310.
[70] A.M. Bayoumy, A. Refaat, I.S. Yahia, H.Y. Zahran, H. Elhaes, M.A. Ibrahim, M. Shkir, Functionalization of graphene quantum dots (GQDs) with chitosan biopolymer for biophysical applications, Opt. Quant. Electron. 52 (1) (2020), https://doi.org/10.1007/s11082-019-2134-z.
[71] A. Omar, H. Ezzat, H. Elhaes, M.A. Ibrahim, Molecular modeling analyses for modified biopolymers, Biointerface Res. Appl. Chem. 11 (1) (2021) 7847–7859.
[72] H. Ezzat, A.A. Menazea, W. Omara, O.H. Basyouni, S.A. Helmy, A.A. Mohamed, W. Tawfik, M. Ibrahim, DFT:B3LYP/ LANL2DZ study for the removal of Fe, Ni, Cu, As, Cd and Pb with Chitosan, Biointerface Res. Appl. Chem. 10 (6) (2020) 7002–7010.
[73] A. Refaat, M.A. Ibrahim, H. Elhaes, R. Badry, H. Ezzat, I.S. Yahia, H.Y. Zahran, M. Shkir, Geometrical, vibrational, and physical properties of polyvinyl chloride nanocomposites: molecular modeling approach, J. Theor. Comput. Chem. 18 (8) (2020) 1950037.
[74] Frisch, M. J. E. A., Trucks, G. W., Schlegel, H. B., Scuseria, G. E., Robb, M. A., Cheeseman, J. R., ... & Nakatsuji, H. (2014). Gaussian~ 09 Revision D. 01.
[75] A.D. Becke, Density-functional thermochemistry. III. The role of exact exchange, J. Chem. Phys. 98 (1993) 5648.
[76] C. Lee, W. Yang, R.G. Parr, Development of the Colle-Salvetti correlation-energy formula into a functional of the electron density, Phys. Rev. B 37 (2) (1988) 785–789.
[77] B. Miehlich, A. Savin, H. Stoll, H. Preuss, Results obtained with the correlation energy density functionals of becke and Lee, Yang and Parr, Chem. Phys. Lett. 157 (3) (1989) 200–206.
[78] A. Abbasi, J.J. Sardroodi, Interaction of sulfur trioxide molecules with armchair and zigzag stanene-based nanotubes: electronic properties exploration by DFT calculations, Adsorption 24 (5) (2018) 443–458.
[79] A. Abbasi, DFT study of the effects of Al P pair doping on the structural and electronic properties of stanene nanosheets, Physica E 108 (2019) 34–43.
[80] A. Abbasi, J.J. Sardroodi, Electronic structure tuning of stanene monolayers from DFT calculations: effects of substitutional elemental doping, Appl. Surf. Sci. 456 (2018) 290–301.
[81] A. Abbasi, J.J. Sardroodi, Structural and electronic properties of group-IV tin nanotubes and their effects on the adsorption of SO 2 molecules: Insights from DFT computations, J. Appl. Phys. 124 (16) (2018) 165302, https://doi.org/10.1063/1.5045674.
[82] M. Ibrahim, E. Koglin, Vibrational spectroscopic study of acetate group, Acta Chim. Slov. 51 (3) (2004) 453–459.
[83] M. Ibrahim, H. Elhaes, Computational spectroscopic study of copper, cadmium, lead and zinc interactions in the environment, Int. J. Environ. Pollut. 23 (4) (2005) 417, https://doi.org/10.1504/IJEP.2005.007604.
[84] M. Ibrahim, A.-A. Mahmoud, Computational notes on the reactivity of some functional groups, J. Comput. Theor. Nanosci. 6 (2009) 1523–1526.
[85] A.M. Bayoumy, M. Ibrahim, A. Omar, Mapping molecular electrostatic potential (MESP) for fulleropyrrolidine and its derivatives, Opt. Quant. Electron. 52 (7) (2020), https://doi.org/10.1007/s11082-020-02467-6.
[86] A.M. Bayoumy, H. Elhaes, O. Osman, T. Hussein, M.A. Ibrahim, Mapping molecular electrostatic potential for heme interacting with nano metal oxides, Biointerface Res. Appl. Chem. 10 (2) (2020) 5091–5095.